

First-principles study of Se-intercalated graphite

M. Bartkowiak^{1,2}, N.A. Modine³, J.O. Sofo⁴, and G.D. Mahan¹

(1) *Department of Physics and Astronomy, University of Tennessee, Knoxville, TN 37996-1200,*

and

Solid State Division, Oak Ridge National Laboratory, Oak Ridge, TN 37831-6030

(2) *Institute of Physics, A. Mickiewicz University, ul. Umultowska 85, 61-614 Poznań, Poland*

(3) *Sandia National Laboratories, Albuquerque, NM 87185-1421*

(4) *Centro Atómico Bariloche and Instituto Balseiro, (8400) Bariloche, RN, Argentina*

(April 15, 2000)

Abstract

Se-intercalated graphite compounds (Se-GICs) are considered as promising candidates for room-temperature thermoelectric cooling devices. Here we analyze the crystallographic structure and electronic properties of these materials within the framework of density-functional theory. First, the Adaptive-Coordinate Real-space Electronic Structure (ACRES) code is used to determine the stable structure of a representative stage-2 Se-GIC by relaxing atomic positions. The stable configuration is found to be a pendant-type structure, in which each selenium is bonded covalently to two atoms within the same carbon layer, causing a local distortion of the in-plane conjugation of the graphite. Then, we use the full potential linearized augmented plane wave (FP-LAPW) method to calculate the electronic band structure of the material and discuss its properties. Near the Fermi energy E_F , there are wide bands originating from the host graphitic electronic structure and a few very narrow

RECEIVED
JUN 06 2000
OSTI

DISCLAIMER

This report was prepared as an account of work sponsored by an agency of the United States Government. Neither the United States Government nor any agency thereof, nor any of their employees, make any warranty, express or implied, or assumes any legal liability or responsibility for the accuracy, completeness, or usefulness of any information, apparatus, product, or process disclosed, or represents that its use would not infringe privately owned rights. Reference herein to any specific commercial product, process, or service by trade name, trademark, manufacturer, or otherwise does not necessarily constitute or imply its endorsement, recommendation, or favoring by the United States Government or any agency thereof. The views and opinions of authors expressed herein do not necessarily state or reflect those of the United States Government or any agency thereof.

DISCLAIMER

**Portions of this document may be illegible
in electronic image products. Images are
produced from the best available original
document.**

bands mainly of Se $4p$ character. The latter bands contribute to high peaks in the density of states close to E_F . We show that this feature, although typical of many good thermoelectrics, does not necessarily imply high thermopower in the case of Se-GICs.

PACS numbers: 71.15.Nc, 71.20.Tx, 74.25.Fy

Typeset using REVTEX

I. INTRODUCTION

Graphite intercalation compounds (GICs) are formed by insertion of atomic or molecular layers of a different chemical species, called the *intercalant*, between the layers of a graphitic host material (see Ref. 1 for a review). Traditionally, GICs are produced by diffusing the intercalant into a pre-existing graphitic host. Recently, however, chemical vapor deposition (CVD) was proposed as a new method to produce GICs.^{2,3} In CVD, the intercalants are captured between the graphite layers during growth, so that the diffusion kinetics are no longer a limiting factor. Many new GICs have been obtained in this way.²⁻⁴ Some of them are reported in a patent by the Sharp Corporation² to exhibit unusually high thermoelectric power S , relatively high electrical conductivity σ , and quite low thermal conductivity κ . These properties make the CVD-grown GICs very promising materials for room-temperature ($T \sim 300$ K) thermoelectric cooling devices. The overall performance of a thermoelectric device can be expressed as a function of the dimensionless figure of merit,

$$ZT = \frac{S^2 \sigma}{\kappa} T, \quad (1)$$

which describes the interplay between Peltier cooling at the junctions, Joule heating in the material, and the back heat flow from the hot to the cold junctions. The best currently known thermoelectric materials exhibit $ZT \sim 1$, and the efficiency of conventional gas-compression-based cooling devices corresponds to $ZT \sim 4$. On the other hand, in Ref. 2, experimental values of $ZT > 30$ are reported for Se- and Te-GICs. If this result could be confirmed, these materials not only would represent a major breakthrough in the field of thermoelectrics, but they also would revolutionize the cooling and power generation industries and related technologies.

An independent study of Se-GICs is reported in Ref. 4. The authors describe their synthesis process (also CVD based) and their characterization of the resulting materials. X-ray diffraction (XRD), X-ray photoemission spectroscopy (XPS), and Raman scattering were used to obtain some data on the crystallographic and electronic structures of the materials.

Electrical resistivity and thermoelectric measurements in the direction perpendicular to the carbon layers showed that the produced Se-GICs indeed had very high Seebeck coefficients S , but they were at least a factor of 10 smaller than those reported by the Sharp Corporation.^{2,3}

Here we study the properties of a representative Se-GICs within the framework of the density-functional theory (DFT). Our procedure is first to find the crystallographic structure of the material, which is not fully determined by available experimental data, and then to calculate the electronic band structure and investigate its properties and their implications for thermoelectric performance.

The available experimental data about the structure of Se-GICs is reviewed in Sec. II, along with several proposed bonding mechanisms. In the process, we identify a set of issues that we wish to resolve using our first-principles treatment.

In Sec. III, the stable positions of the atoms are found for a representative Se-GIC using the Adaptive Coordinate Real-Space Electronic Structure (ACRES) code developed at Harvard University.⁵ ACRES is designed to perform DFT total energy calculations for atoms, molecules, bulk solids, and surfaces on parallel computers, and it offers efficient computation of *ab initio* forces and treatment of low symmetry systems. Calculations are performed in real space on a grid, whose resolution is adapted locally to the requirements of a given system. Sparsity of the DFT Kohn-Sham Hamiltonian in real space and load balancing resulting from the adaptive mesh make ACRES an excellent technique for use on parallel computers. *Ab initio* pseudopotentials are used to represent the interaction between nuclei and electrons. The relaxation is performed by moving the atoms based on the computed forces until a local minimum of the energy is found.

Sec. IV discusses the calculation of the electronic band structure using WIEN97 (Ref. 6), a self-consistent Full-Potential Linearized Augmented Plane Wave (FP-LAPW) software package. In brief, this implementation of the DFT efficiently computes the electronic structure, while avoiding the pseudopotential approximation. In addition, it features different possible approximations for the exchange and correlation potential, including the local spin density approximation (LSDA) and generalized gradient approximation (GGA). WIEN97 is

also used to calculate the charge density distribution and to determine the nature of the bonding between selenium and carbon.

We found large asymmetries in the density of states (DOS) of Se-GICs near the Fermi energy. This is typical of many good thermoelectrics. However, in Sec. V, we present a general discussion of the thermoelectric properties of materials with band structures similar to that of Se-GICs, and show that an asymmetric DOS with large variations near the Fermi energy does not necessarily mean that the material will exhibit a high thermopower.

II. STRUCTURE OF SE-GICS

Relatively little is known from experiment about the structure of Se-GICs. A GIC is denoted as stage- n if there are n layers of graphite between each layer of the intercalant. Se-GICs are usually produced as mixtures of stage-2 to stage-5 materials. The only pure compound analyzed in Ref. 4 was the stage-3 GIC corresponding to the chemical composition $C_{24}Se$. Following convention, the direction perpendicular to the carbon layers is taken to be the z direction. In Ref. 4, analysis of the X-ray diffraction patterns in this direction showed that layers of selenium and carbon are stacked as shown in Fig. 1.

In graphite-based materials, there are three possible types of carbon layers corresponding to different x - y positions of the layers. In graphite, usually two of the layer types are alternated in an A-B stacking order. The stacking orders of Se-GICs are unknown. There are two possible basic types of stacking arrangements in GICs: type I where the carbon layers on either side of the intercalant layer are of the same type (A-X-A, where "X" represents the intercalant layer), and type II where they are different (A-X-B). The stacking arrangement is often related to properties of the intercalant — while donor compounds usually exhibit type I arrangement, both types are found in acceptor GICs.¹ Therefore, it is difficult to decide *a priori* which stacking arrangement should be expected in Se-GICs, particularly when the nature of the bonding between Se and the carbon layers is unknown.

Two possible bonding mechanisms were discussed in Ref. 4: ionic and covalent. Accord-

ing to the XRD data on stage-3 $C_{24}Se$, the selenium layers are centered between the two neighboring carbon layers (or very nearly so). Fitting the experimental data to a simple model, in which all layers were presumed to be planar, indicated that the displacement α from the central position should be less than 0.15 Å (see Fig. 1). This result suggests that either the selenium is bonded ionically, or else it is bonded covalently to both neighboring carbon layers forming an interlayer bridge. Since the difference in electronegativity of carbon and selenium is very small, substantial ionic charge transfer between the selenium and carbon layers seems unlikely. However, the distance between the graphite layers is much larger than twice the typical C-Se covalent bond length. Therefore, a stable state in which the Se bridges between adjacent carbon layers also seems unlikely unless it is accompanied by a large local distortion of the graphite planes.

An alternative structural model with covalent C-Se-C bonding is that selenium is bonded to two carbon atoms within the same layer (the pendant model). This possibility is supported by analogy to graphite oxide. Oxygen is chemically similar to selenium, and graphite oxide has a pendant-type structure.^{7,8} Se bound to only one of the carbon layers should be displaced from the central position between the graphite layers. However, without knowing the x - y positions of the Se atoms and the extent of buckling of the carbon layers, it is impossible to estimate the magnitude of this displacement.

III. RELAXATION OF THE STRUCTURE

First-principles calculations provide a powerful tool for distinguishing between alternative structural models such as those mentioned above. Since there are many possible Se-GICs corresponding to different stages, stoichiometries, and stacking orders, it is necessary to choose a representative compound for our calculations. We choose stage-2 $C_{16}Se$, which is the simplest compound that keeps the essential feature of the Se-GICs, a Se layer between two graphite layers, while maintaining the in-layer Se density found in the experimentally identified stage-3 $C_{24}Se$. We expect that the most important features of other Se-GICs are

essentially the same. Moreover, it is likely that stage-2 $C_{16}Se$ has better thermoelectric properties than stage-3 $C_{24}Se$, because its thermal conductivity is expected to be lower.⁹ A type I stacking order (A-Se-A) is chosen because it is hard to explain why we would preferentially observe a stage-3 compound in experiments if the Se preferred to be between A and B layers. Although no crystallographic data is available for this compound, once these basic choices have been made, all structural parameters, including the positions of the Se atoms and the distortion of the carbon layers, are determined by relaxing the structure within a self-consistent computational scheme.

The ACRES code, the local density approximation as parameterized by Perdew and Zunger¹⁰, and the pseudopotentials of Hamann, Schlüter, and Chiang (HSC)¹¹ were used to perform the structural relaxations. The charge distribution of the system was sufficiently uniform that no adaptation of the computational grid was necessary. A $3 \times 3 \times 2$ Monkhorst-Pack k-point grid was used in order to sample the Brillouin zone. The relaxation was performed by computing the forces acting on the nuclei and moving the atoms using a preconditioned steepest descent algorithm until all force components were less than 25 meV/Å. Calculations took a few weeks on 8 processors of a SGI ORIGIN 2000 computer.

As an initial configuration for stage-2 $C_{16}Se$, we put the selenium atom close to the center between the carbon layers, and in a randomly chosen x - y position. The carbon layers were initially taken to be completely flat and separated by the distances measured in Ref. 4 for stage-3 $C_{24}Se$, i.e., 3.4 Å between neighboring graphite layers, and $2 \times 2.69 = 5.38$ Å between carbon layers with Se in between.

About 50 updates of the ionic positions were required to fully relax the atoms into the new configuration shown in Fig. 2. Due to the lack of symmetries during the relaxation, this structure must correspond to a minimum (local or global) of the total energy of the system. Clearly, it is a pendant-type structure with the Se bound to two atoms in a single graphite layer. The distance between the Se and the C-C bond center is 2.02 Å. As expected for this type of structure, the Se atom is displaced significantly ($\alpha = 0.47$ Å) from the center of the interlayer region. Although the graphite layers are quite rigid, the carbon atoms closest

to the Se atom are also significantly displaced (0.16 Å) from the average z position of their layer. As discussed below, this allows for partial sp^3 rehybridization of the carbons and for covalent bonding between the carbons and the selenium.

Next, we unsuccessfully attempted to find any stable or metastable state in which the Se bridges between graphite layers by performing the following calculations: We symmetrized the final configuration obtained above with respect to the central plane of the interlayer region and displaced the Se atom by 0.2 Å in the x - y plane in order to break other symmetries. We then fully relaxed all of the atomic positions subject to the constraint that the Se must be half-way between the carbon layers. During the relaxation, the Se moved from an asymmetric x - y position to a symmetric position between the center of a C-C bond in one graphite layer and the center of a C-C bond in the other graphite layer. In this new structure, the Se atom has 4 nearest neighbor carbon atoms (2 in each layer) that form a 1.43 Å by 4.73 Å rectangle. The average atom in each graphite layer was 2.44 Å from the Se atom, which is substantially shorter than 2.69 Å, the experimental distance found for the stage-3 compound. The interlayer distance in the new structure is presumably the distance at which the forces attempting to reduce the Se-C bond lengths by pulling the layers together are balanced by the Fermi repulsion resulting from the overlap of π bonds on different layers.

In order to distinguish whether the new structure is a minimum or a saddle point of the total energy, we slightly broke its symmetry and removed the constraint on the relaxation. The structure quickly reverted to the pendant-type structure discussed above. This indicates that the new structure is a saddle point between the energy basins associated with the pendant-type structures rather than a true energy minimum. From this, we conclude that the simple geometric argument against a bridging structure (the distance between the graphite layers is much larger than twice the typical C-Se bond length) seems to hold true even in the presence of the substantial layer corrugations induced by the Se atoms.

The energy of the saddle point found above gives a 152 meV energy barrier for conver-

sion between a pendant-type structure with Se bound to one layer and the corresponding structure with Se bound to the other layer. Even considering that the attempt rate is likely to be unusually small due to the relatively weak bonding between the Se and the graphite layers, this suggests that the Se atoms should fluctuate between the two equivalent versions of the pendant-type structure at a rate of perhaps 10^5 Hz at room temperature. This value is very rough approximation — among many details left out of the model, the Se atoms will certainly not fluctuate coherently and the graphite layers will not fully relax to accommodate the Se at the saddle point. However, given this barrier, it would be surprising if the Se atoms did not fluctuate at some rather significant rate. Therefore, we suggest the experimental evidence that the Se is very near the center of the interlayer region could instead be explained by a picture in which the Se atoms are fluctuating rapidly between two sites 0.47 Å from the center. Such fluctuations should lead to large, anisotropic Debye-Waller factors in the diffraction data, but we have been unable to verify this prediction since, to our knowledge, Debye-Waller factors have not been measured for Se-GICs.⁹

It is clear from our calculations that the Se atoms want to be located over the centers of graphite bonds. This can be understand as follows. The Se atoms want to be where the electron density is high, but they can not get too close to the C atoms. In graphite, this means that they want to sit in the lobes of the π orbitals. With a type II stacking order (A-Se-B), the minimum distance between the bond centers in different graphite layers is larger than the corresponding distance in type I structures. Since the main problem in forming Se-GICs with bridging Se atoms seems to be that this distance is too large, we seem justified in assuming that the stable configuration would have a pendant-type structure even with a type II stacking order.

IV. BAND STRUCTURE

Now that the stable crystallographic structure has been identified, we analyze the nature of the Se-C bonding, the band structure of the material, and its electronic properties using a

related first-principles technique. The band structure of the relaxed pendant-type structure of stage-2 $C_{16}Se$, which forms a hexagonal lattice with 17 (9 nonequivalent) atoms per unit cell, was calculated within the FP-LAPW method.⁶ The Kohn-Sham equations are solved using a basis of linearized augmented plane waves.¹² Exchange and correlation potentials are included within the GGA of Perdew, Burke, and Ernzerhof.¹³ We use a well converged basis set of about 24000 plane waves and a 600 point sampling of the Brillouin zone (BZ), which corresponds to 275 points in the irreducible wedge (IBZ). The muffin-tin radii are taken as 1.3 Bohr for C and 2.0 Bohr for Se, respectively.

The band structure of the relaxed $C_{16}Se$ is shown in Fig. 3. Distortion of the graphite planes leads to a significant reduction of the symmetry of the structure compared to that of pure hexagonal graphite, and causes the appearance of many carbon-type bands. However, the main features of the graphitic band structure are still identifiable in the band structure of relaxed $C_{16}Se$. In particular, the crossing of bands at the K point, which is characteristic of graphite, is still present here. The crossing bands are associated with the π orbitals of carbons in the layer that does not bond to selenium. This layer remains essentially flat and maintains a graphite-like character. However, if the dynamical picture of Se atoms resonating between positions close to the two neighboring carbon layers is true, then both layers should be distorted to some extent, and one may expect a gap to open at the Fermi energy E_F . The same conclusion follows even when the resonating motion of the Se atoms is suppressed by very low temperatures. In this case, a portion of the Se atoms can be expected to bond to each plane, either in an ordered or disordered fashion. Since both layers have π orbitals involved in bonding to Se, a small gap should be opened for both carbon planes, and the characteristic graphitic band crossing should be eliminated. We have checked this point by calculating the band structure of $C_{16}Se$ with a reduced distance between flat graphite planes and a centered selenium atom. In this configuration, the Se atoms perturb the carbon orbitals in both layers, and the band structure exhibits a small gap (about 0.02 eV) at the Fermi energy.

There are two sets of bands that have primarily Se character. One group is located

around -14 eV to -12 eV and corresponds to Se-*s* orbitals. The second group, mainly of Se-*p* character, lies in close vicinity to E_F . There are two flat bands of this kind right below the Fermi energy. Also, the bands right above E_F are a mixture of Se-*p*, and C-*p* states. These narrow bands contribute to high peaks in the density of states (DOS), as shown in Fig. 4. As a result, the DOS is quite asymmetric at E_F . Furthermore, due to the low DOS at E_F , it is easy to imagine that even a small amount of doping or a minor change in ordering might shift the Fermi energy near enough to the Se-*p*-related spike to generate an enormous DOS asymmetry at E_F .

The calculated spatial distribution of the charge density shows that there is very little charge transfer between the graphite sheets and the intercalant. There is some charge accumulation at the spaces between the Se atom and the two neighboring carbons, indicating covalent bonding. This covalent bonding correlates with the buckling of the graphite planes close to the intercalated selenium. The two carbon atoms bound to selenium adopt partial sp^3 hybridization and force the buckling of the plane.

V. ELECTRONIC AND THERMAL PROPERTIES

As discussed in Sec. IV, bonding of selenium to the graphite planes is likely to cause a gap in the band structure at the Fermi energy E_F . This is consistent with the experimental data for the resistivity — the *z*-axis resistivity of Se-GICs is two order of magnitude higher than that of CVD grown graphite.⁴ A similar situation has been found in graphite oxide, where puckered graphite layers result in insulating behavior.⁷ A small temperature dependence of the resistivity is also in agreement with this scenario.

When searching for good thermoelectric materials, it is usually accepted that an asymmetric DOS with large variations near the Fermi energy will produce high thermopower. While this is true when there is only one band (or a few bands of similar or mixed type) participating in the electronic transport processes, it may be misleading when the DOS comes from very different bands. For example, in our case, there is a large asymmetry in DOS

coming from the localized Se-*p* orbitals. This high DOS is superimposed on the pseudogap originating from the host graphitic electronic structure. The resulting total DOS, although highly asymmetric, does not necessarily produce a high thermopower. The reason is as follows: Let us consider a system where the transport properties are determined by two bands. Just as for the case of Se-GICs, let us assume that one of these bands is a wide band that contributes a high conductivity σ_1 , and that would correspond to a small thermopower S_1 . On the other hand, let the other band be a narrow band with a small contribution σ_2 to the conductivity, and one that would give a high thermopower S_2 . We have $\epsilon_\sigma \equiv \sigma_2/\sigma_1 \ll 1$ and $\epsilon_S \equiv S_1/S_2 \ll 1$. As it is well known,¹⁴ the electrical conductivity is simply the sum of the conductivities for the separate bands,

$$\sigma = \sigma_1 + \sigma_2 , \quad (2)$$

whereas the Seebeck coefficient of the system reads

$$S = \frac{S_1\sigma_1 + S_2\sigma_2}{\sigma_1 + \sigma_2} = \frac{S_2(\epsilon_\sigma + \epsilon_S)}{1 + \epsilon_\sigma} . \quad (3)$$

It is seen that the thermopower remains small — it is of order of S_1 , i.e., of order of that for the wide band. From the point of view of improving thermoelectric properties, we do not gain much by combining bands with different transport coefficients.

It is interesting to note that if the above scenario of Se atoms fluctuating between two equivalent versions of the pendant-type structure is indeed true, it should provide a strong phonon scattering mechanism. The high relative mass of Se should enhance scattering, while the Se-induced distortion of the graphite layers indicates that there must be significant coupling between the Se atoms and the phonon modes of the layers. Furthermore, since the distance between graphite planes is almost doubled by Se intercalation, thermal conduction in the *z* direction should be mediated by the Se atoms. The situation may be similar to that of “rattling” semiconductors such as filled skutteredites¹⁵ or clathrates,¹⁶ and one could expect that the lattice thermal conductivity of Se-GICs would be greatly reduced as compared to that of pure graphite. This would lead to an enhancement of *ZT* and an

overall improvement of the thermoelectric properties of the material. Experimental data on the thermal conductivity of Se-GICs reported in Ref. 2 supports this conclusion.

ACKNOWLEDGMENTS

Research support is acknowledged from the University of Tennessee, from Oak Ridge National Laboratory managed by Lockheed Martin Energy Research Corp. for the U.S. Department of Energy under contract DE-AC05-96OR22464, and from a Research Grant No. N00014-97-1-0565 from the Applied Research Projects Agency managed by the Office of Naval Research. The ACRES software was developed by the DoD HPCMP CHSSI program, and the structural relaxation calculations were performed using a grant of HPC time from the DoD HPC ARL Major Shared Resource Center. M.B. acknowledges also support from K.B.N Poland, Project Nos. 2 P03B 056 14 and 2 P03B 037 17. J.O.S. is supported by CONICET, Argentina. Sandia is a multiprogram laboratory operated by Sandia Corporation, a Lockheed Martin Company, for the United States Department of Energy under Contract DE-AC04-94AL85000.

REFERENCES

¹ M.S. Dresselhaus and G. Dresselhaus, *Adv. Phys.* **30**, 139 (1981).

² H. Nakaya, Y. Yoshimoto, M. Yoshida and S. Nakajima, European Patent # EP0500359 (1992).

³ Y. Yoshimoto, S. Tomonari, Y. Higashigaki, S. Nakajima and K. Inoguchi, US Patent # US5,273,778 (1993).

⁴ L. Grigorian, S. Fang, G. Sumanasekera, A.M. Rao, L. Schrader and P.C. Eklund, *Synth. Metals*, **87**, 211 (1997).

⁵ N. A. Modine, G. Zumbach, and E. Kaxiras, in E. Kaxiras, J. Joannopoulos, P. Vashishta, and R. Kalia (eds.), *Materials Research Society Proceedings 408*, Material Research Society, Pittsburgh, PA, 1996, p. 139; G. Zumbach, N.A. Modine, and E. Kaxiras, *Solid State Commun.* **99**, 57 (1996); N.A. Modine, G. Zumbach, and E. Kaxiras, *Phys. Rev. B* **55**, 10289 (1997).

⁶ P. Blaha, K. Schwarz, and J. Luitz, WIEN97, Vienna University of Technology, 1997. (Improved and updated Unix version of the original copyrighted WIEN-code, which was published by P. Blaha, K. Schwarz, P. Soratin, and S.B. Trickey, in *Comput. Phys. Commun.* **59**, 399 (1990)).

⁷ G.R. Hennig, in *Progress in Inorganic Chemistry*, ed. F.A Cotton, v. 1, Interscience Publishers Inc., New York, 1959, p. 125.

⁸ T. Nakajima and Y. Matsuo, *Carbon* **32**, 469 (1994).

⁹ P.C. Eklund, private communication.

¹⁰ J.P. Perdew and A. Zunger, *Phys. Rev. B* **23**, 5048 (1981).

¹¹ D. R. Hamann, M. Schlüter, and C. Chiang, *Phys. Rev. Lett.* **43**, 1494 (1979).

¹² D. Singh, *Plane Waves, Pseudopotentials, and the LAPW Method* (Kluwer Academic, New

York, 1994).

¹³ J.P. Perdew, S. Burke and M. Ernzerhof, Phys. Rev. Lett. **77**, 3865 (1996).

¹⁴ H. J. Goldsmid, *Thermoelectric Refrigeration* (Plenum Press, New York, 1964).

¹⁵ B.C. Sales, D. Mandrus and R.K. Williams, Science **272**, 1325 (1996).

¹⁶ G. S. Nolas, J. L. Cohn, G. A. Slack, and S. B. Schujman, Appl. Phys. Lett. **73**, 178 (1998).

FIGURES

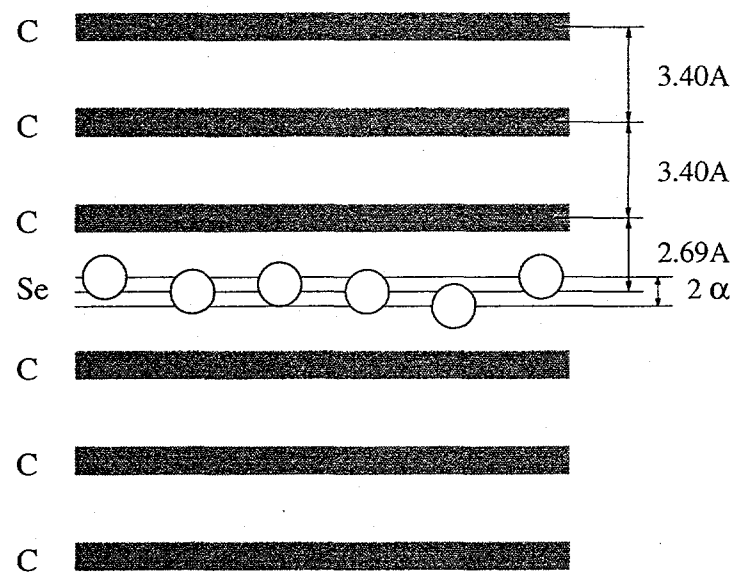


FIG. 1. Stacking of carbon and selenium layers along the z direction for stage-3 C_{24}Se (From Ref. 4).

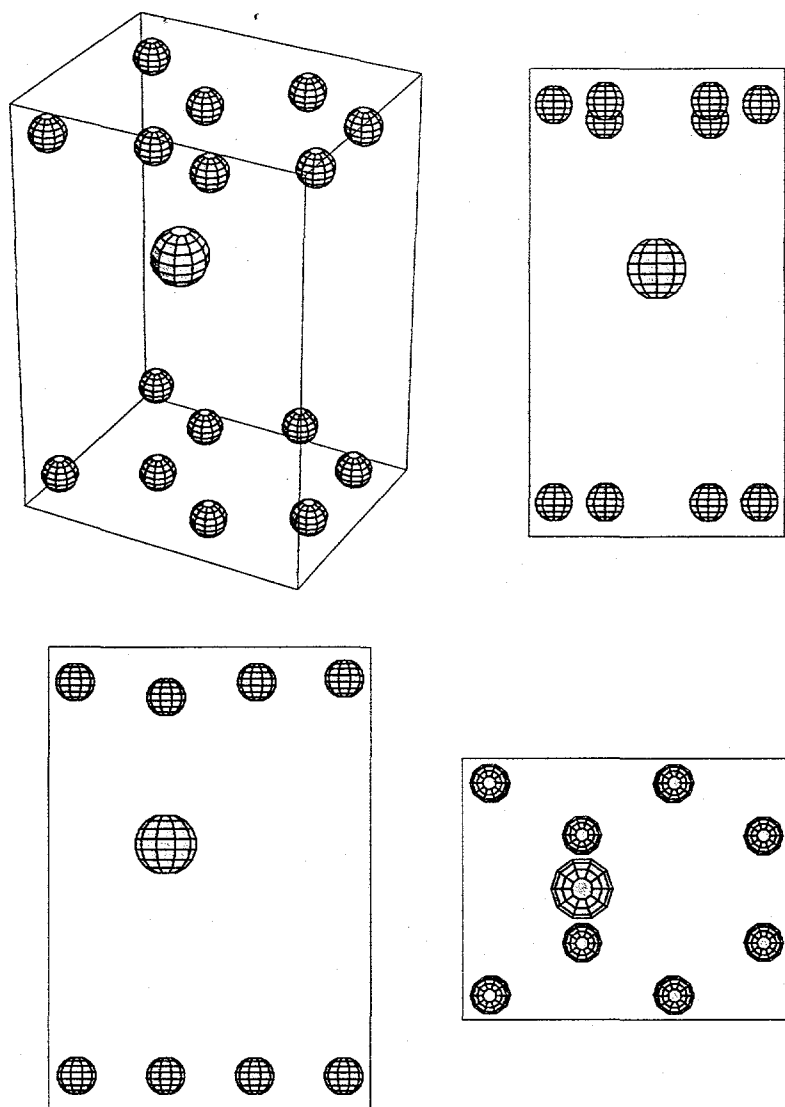


FIG. 2. Perspective view and projections along the x , y and z directions of the stable pental-tetrahedral structure of stage-2 C_{16}Se obtained by relaxing atomic positions.

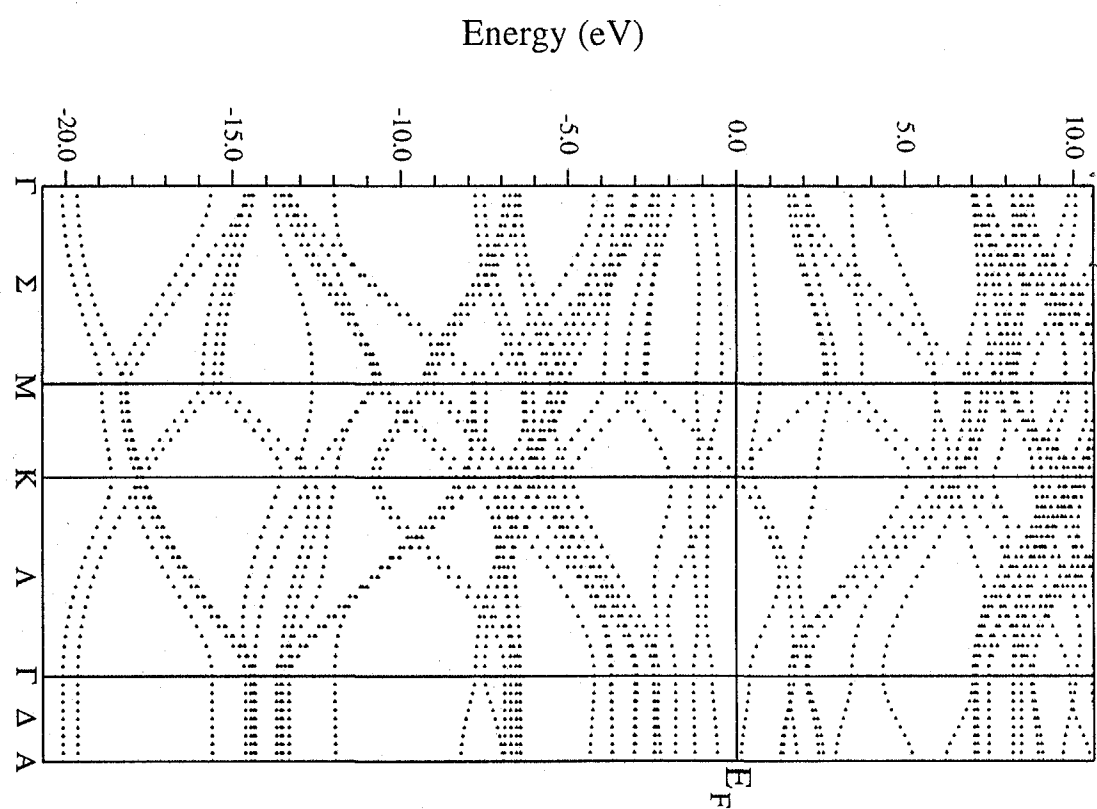


FIG. 3. Electronic band structure of stage-2 C₁₆Se in the stable pendant-type structure along a path between symmetry points of the Brillouin zone.

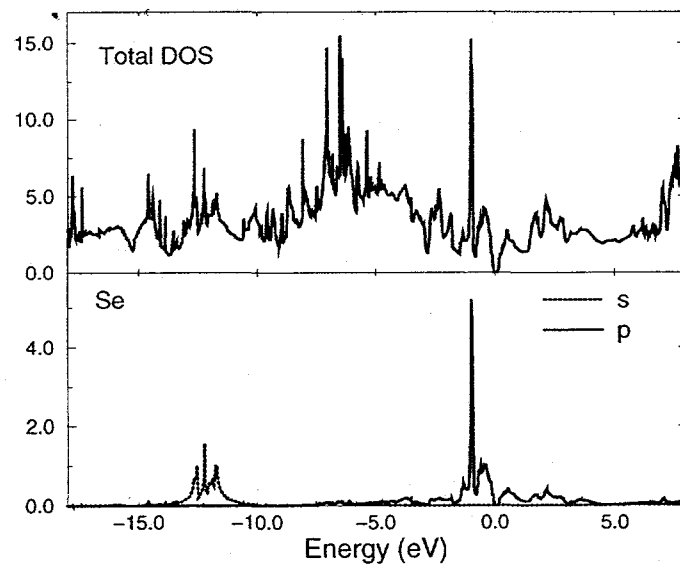


FIG. 4. Electronic density of states of stage-2 $C_{16}Se$ in the stable pendant-type structure as a function of energy measured from the Fermi level. The lower panel shows contributions from the bands of primarily Se-4s and Se-4p character.